

NONLINEAR SEISMIC ANALYSIS OF A CONCRETE ARCH BRIDGE WITH STEEL WEBS

H. Yuan, Q. Wu, B. Chen

College of Civil Engineering, Fuzhou University, Fuzhou, CHINA.

e-mails: yuanhh@fzu.edu.cn, wuqingx@fzu.edu.cn, baochunchen@fzu.edu.cn

SUMMARY

In this study, three finite element (FE) models for arch bridges respectively with conventional RC web, corrugated steel web, and plain steel web are established by using nonlinear FE program NL Beam3D, and their nonlinear seismic responses are also investigated. When subjected to longitudinal seismic excitations, all three arch bridges remain in elastic state and the axial force and in-plane bending moment are predominant. However, when subjected to transverse seismic excitations, the seismic responses of all three bridge models are greater than those under longitudinal excitations, and the arch springing will enter the plastic stage, the predominant internal forces change to the axial force and out-of-plane bending moment. The arch bridge with steel webs shows better seismic performance than conventional concrete arch bridge with RC web.

Keywords: *Arch bridges, composite structure, corrugated steel webs, plain steel webs, nonlinear seismic response.*

1. INTRODUCTION

Concrete arch bridge with steel webs is a modified type bridge to replace reinforced concrete webs (RCW) in conventional concrete arch bridge with corrugated steel webs (CSW) or plain steel webs (PSW) [1]. The elevations and cross sections of RC-CSW arch rib and RC-PSW arch rib are respectively shown in Fig. 1 and 2. In comparison with the conventional concrete arch bridge, these two types of composite arch rib have several advantages such as less deadweight, more convenient construction, lower cost and shorter construction period. It is expected that steel webs will find wide applications in long-span RC arch bridges.

In previous studies [2, 3] of trial-design on Lingdou Bridge, a 160 m-span concrete arch bridge in Fujian Province, China, the replacement of concrete webs with steel webs can effectively reduce the deadweight by approximately 30%, and consequently decrease the internal force to some extent. From the elastic seismic analysis of a RC-CSW arch bridge [1], it is clearly shown that the seismic performances of RC-CSW arch bridge are better than those of conventional RC bridge.

However, the nonlinearity of materials and geometry, which is supposed to have a considerable influence on the elastic-plastic seismic responses of long-span arch bridges, has not been adequately addressed in above mentioned studies. Therefore, in order to clarify the influence of different web types on the nonlinear seismic performance of

long-span concrete arch bridges, according to the previous trail-design studies [1-3], three FE models for arch bridges respectively with RC web, corrugated steel web, and plain steel web are established by using nonlinear FE program *NL_Beam3D* [4-6], and their nonlinear seismic responses are also investigated in this study.

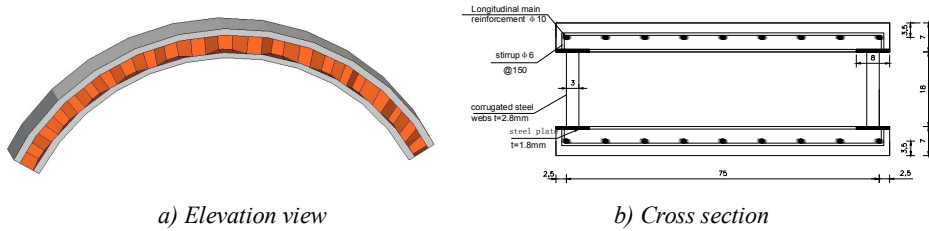


Fig. 1. Schematic diagram of RC-CSW arch rib.

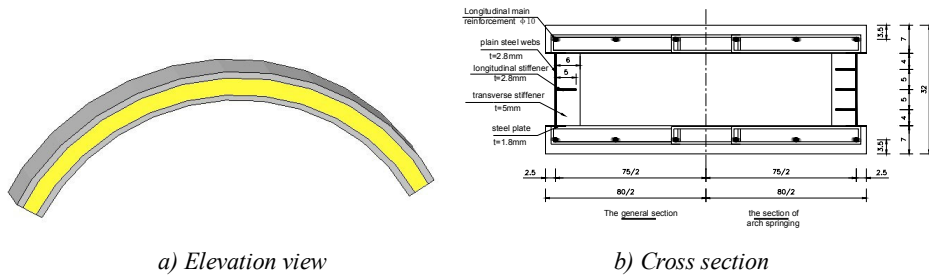


Fig. 2. Schematic diagram of RC-PSW arch rib.

2. FINITE ELEMENT MODELS AND COMPUTATIONAL PROCEDURES

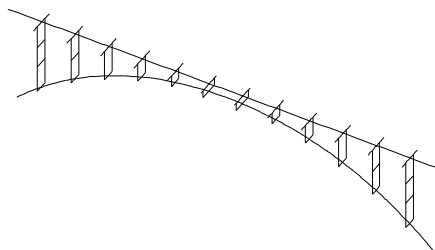
2.1. Analytical model

Three spatial beam-element models for arch bridges adopting different types of web are established according to the aforementioned Lingdou Bridge as shown in Fig. 3a, of which the main span is 160 m, the rise-to-span ratio is 1/4, and the arch-axis coefficient of catenary arch axis is 2.114. All the three FE models are developed by nonlinear finite element program *NL_Beam3D* [4-6]. Since the structural configuration of three models are almost the same except their cross sections of arch ribs, only one beam-element model is shown in Fig. 3b due to space limitations.

The arch ribs, columns and decks of three arch bridges adopt the fibre element model, which can fully take the nonlinear relationship between the axial force and bi-directional bending moment into account. Referred to the Specification for Highway Bridges in Japan [7], bi-linear model is used to simulate the constitutive relation of steel, in which the stiffness after yield is set to be 1/100 of elastic modulus, while a quadratic parabola model for the constitutive relation of concrete material is adopted, which ignores the tensile stress and decrease of compressive stress.



a) Actual bridge photo

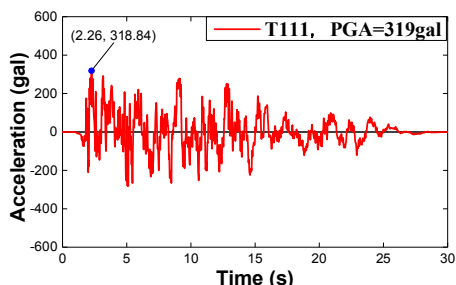


b) Finite element model

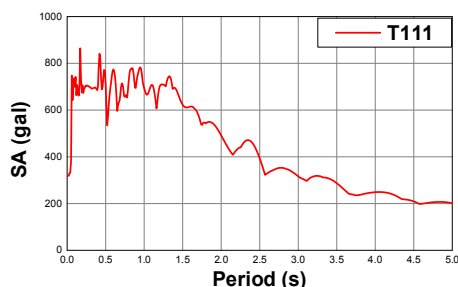
Fig. 3. Lingdou Bridge.

2.2. Computational procedure

As shown in Figure 4, the input ground motion named T111 for time history analysis is a recommended standard seismic wave of Ground Type I, i.e. hard foundation, according to the Specification for Highway Bridges in Japan [7]. The initial stress of the arch bridges is assumed to be under dead load condition [8]. Considering $P-\Delta$ effect, the geometric nonlinearity in computational procedure is evaluated by using moving coordinate method. Subspace iteration method is used to obtain the eigenvalues of natural vibration problem, and time history method to analyse the nonlinear seismic responses. Rayleigh damping model is adopted with damping ratio $\zeta = 0.02$ and the structural frequencies are required to change to different values depending on the direction of ground motion.



a) Acceleration time history



b) Absolute acceleration response spectrum

Fig. 4. Seismic acceleration wave of T111.

3. RESULTS AND DISCUSSION

3.1. Natural vibration analysis

The three arch bridges present the same vibration modes, and the first two modes of in-plane and out-of-plane vibrations are illustrated in Fig. 5. The 1st mode of out-of-plane vibration is symmetric whereas the 1st mode of in-plane vibration mode is antisymmetric

in vertical direction. Fig. 6 compares vibration frequencies among the three arch bridges. In comparison with conventional RC arch bridge, the natural frequencies corresponding to the 1st and 2nd modes of out-of-plane vibration have decreased by 26% and 55% for RC-CSW arch bridge, and by 9% and 7% for RC-PSW arch bridge, respectively, which suggest weaker out-of-plane stiffness of arch bridges with steel webs. However, for in-plane vibration frequencies, there is not much difference among the three arch bridges, which indicates that the change of web type of arch rib has little effect on the in-plane stiffness of arch bridge.

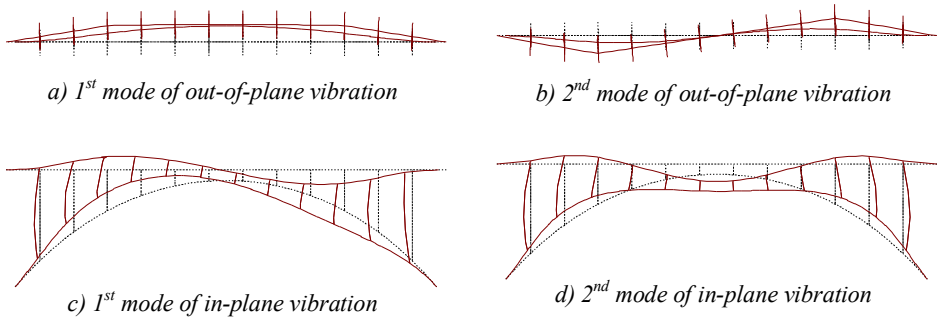


Fig. 5. Main vibration modes for three arch bridges.

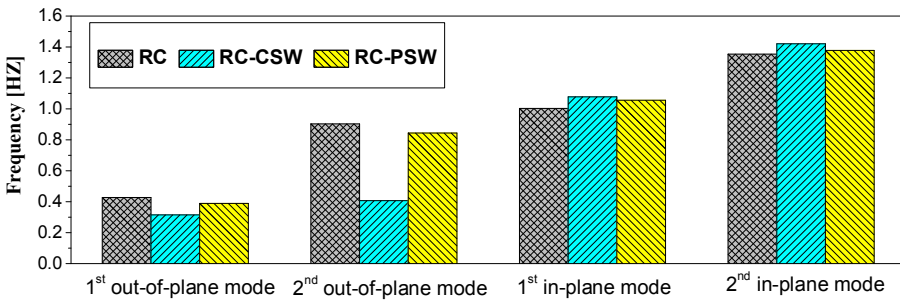


Fig. 6. Comparison of vibration frequencies.

3.2. Nonlinear time-history analysis

3.2.1. Structural response under transverse seismic excitation

Under transverse seismic excitation, the time-history curves of predominant internal forces such as the axial force and the out-of-plane bending moment at arch springing section, where is expected to be potential plastic-hinge region, of three arch bridges are depicted in Fig. 7. By comparison, it can be found that the replacement of RC web by steel webs leads to much smaller internal forces in the earthquake, such as out-of-plane shearing force and axial force. Compared with those of RC arch bridge, the maximum of out-of-plane shearing force and axial force for RC-CSW arch bridge are respectively reduced by 51% and 19%, while for RC-PSW arch bridge by 31% and 18%,

respectively. On the other hand, in comparison with that of RC arch bridge, the maximum of out-of-plane bending moment for RC-CSW arch bridge has not declined, while for RC-PSW arch bridge it has even increased by 22%.

The correlation curves of axial force versus out-of-plane bending moment at arch springing section are plotted in Fig. 8, where the out-of-plane bending moment of inner and outer envelope curves are determined when under predefined axial force the fibre strain of steel reinforcement and concrete at the outermost edge of cross section reaches the corresponding yield strain, respectively. As seen from Fig. 8, for all the three arch bridges subjected to transverse seismic excitation the small axial forces and large out-of-plane bending moments at arch springing sections have caused the stain of steel reinforcement or concrete at the outermost edge to exceed the yield strain, indicating that the arch springing section enters an elastoplastic state.

The peak strains at the arch springing sections of three arch bridges under transverse seismic excitations are shown in Tab. 1. It is obvious that the conventional RC arch bridge produces the largest stain, $\varepsilon_{RC} = 0.0161$, among the three, followed by the RC-CSW arch bridge, $\varepsilon_{RC-CSW} = 0.0109$, and the RC-PSW arch bridge, $\varepsilon_{RC-CSW} = 0.0078$, being 68% and 49% of that of the RC arch bridge, respectively.

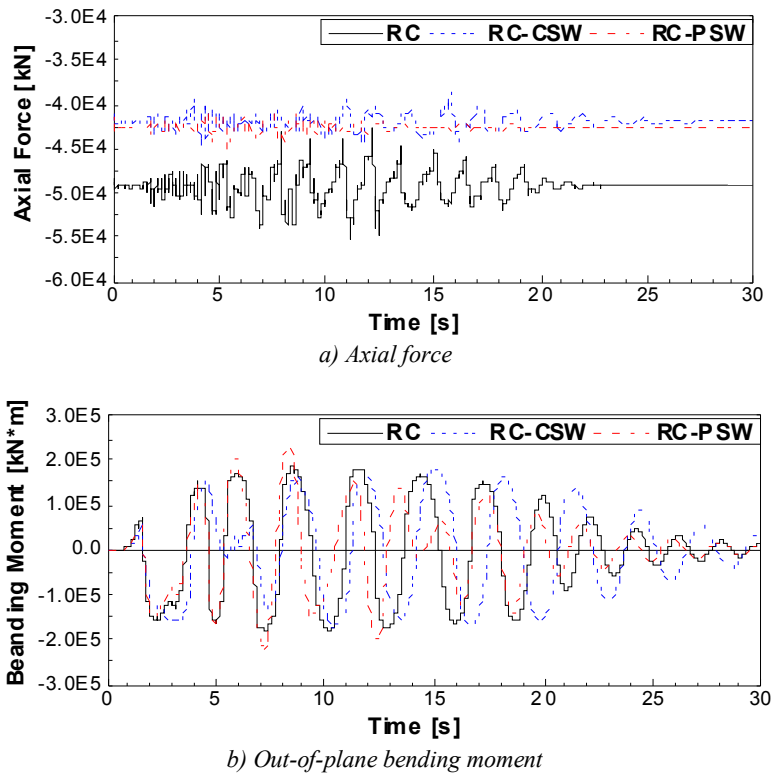


Fig. 7. Time history curves of internal forces at arch springing under transverse earthquake.

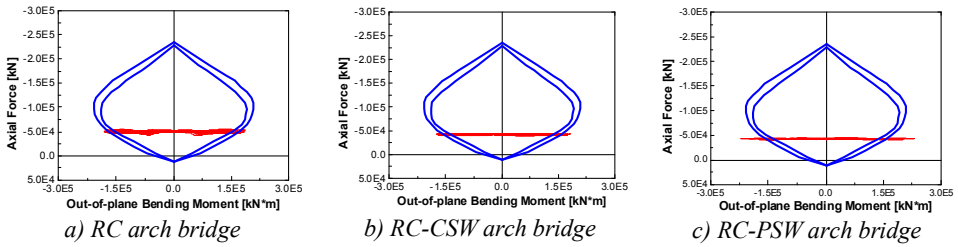


Fig. 8. Correlation curves of $N-M_y$ at arch springing section under transverse earthquake.

Table 1. Comparison of the peak strain at the arch springing section.

Seismic direction	ϵ_{RC}	ϵ_{RC-CSW}	ϵ_{RC-PSW}	$\epsilon_{RC-CSW}/\epsilon_{RC}$	$\epsilon_{RC-PSW}/\epsilon_{RC}$
Transverse	0.0161	0.0109	0.0078	0.68	0.49
Longitudinal	0.0011	0.0006	0.0005	0.55	0.45

Fig. 9 compares the maximum and minimum of transverse displacement response of arch rings that occurs in the transverse earthquake among the three arch bridges. It can be observed from the figure that the transverse displacement response have decreased to some extent after the replacement of concrete webs with steel webs in RC arch bridges. Take the transverse displacement response at the vault as example, the maximum values for RC-CSW and RC-PSW arch bridges are 1.572 m and 1.315 m, respectively, which are 95% and 79% of 1.658 m for conventional RC arch bridge, respectively. The difference of transverse displacement response may be well related to the different natural vibration characteristics among the three arch bridges.

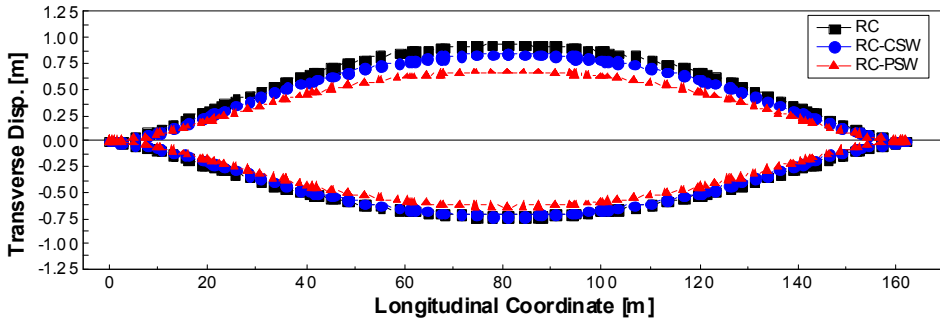


Fig. 9. Extremum of transverse displacement response of arch ring under transverse earthquake.

3.2.2. Structural response under longitudinal seismic excitation

The time-history curves of predominant internal forces, i.e., the axial force and in-plane bending moment, at arch springing section under longitudinal seismic excitation are depicted in Fig. 10. In comparison with the results of RC arch bridge, the maximum values of in-plane bending moment, vertical shearing force and axial force have fallen by 4%, 33% and 14% for RC-CSW arch bridge, and by 7%, 50% and 9% for RC-PSW arch

bridge, respectively. Moreover, the in-plane bending moments under longitudinal seismic excitation are much lower than the out-of-plane bending moments under transverse seismic excitation although the same ground motion is used for both cases.

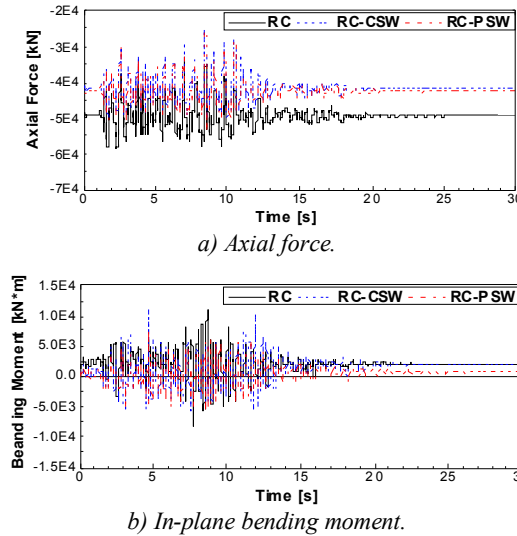


Fig. 10. Time history curves of internal forces at arch springing under longitudinal earthquake.

The correlation curves of axial force versus in-plane bending moment at arch springing section are plotted in Fig. 11, where the in-plane bending moment of inner and outer envelope curves are determined by the same method as stated in Section 3.2.1. It can be seen from Fig. 11 that for all the three arch bridges under longitudinal seismic excitation the arch springing section remain in the elastic state. The peak strains at the arch springing sections of three arch bridges under longitudinal seismic excitations are also listed in Tab. 1. It shows that none of the three arch bridges have reached the elastoplastic state and the seismic responses under longitudinal seismic excitations are much lower than those under transverse seismic excitations. Moreover, the smaller seismic responses of RC-CSW and RC-PSW arch bridges suggest the better seismic performances than conventional RC arch bridge.

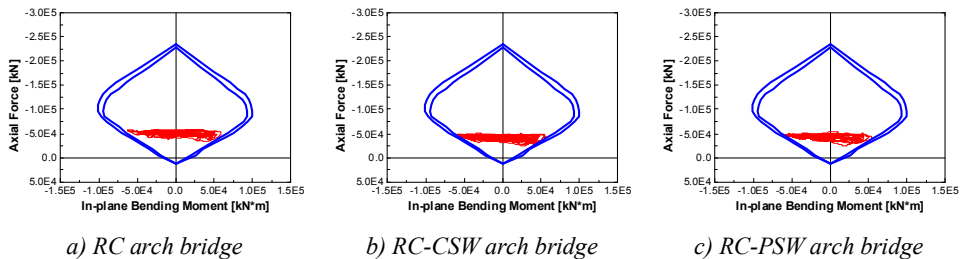


Fig. 11. Correlation curves of N-M at arch springing section under longitudinal earthquake.

Fig. 12 compares the extreme values of longitudinal and vertical displacement responses of arch rings under longitudinal seismic excitations. The three arch bridges have almost the same in-plane displacement responses, indicating the replacement of concrete webs with steel webs in RC arch bridges has a small impact on the structural in-plane stiffness.

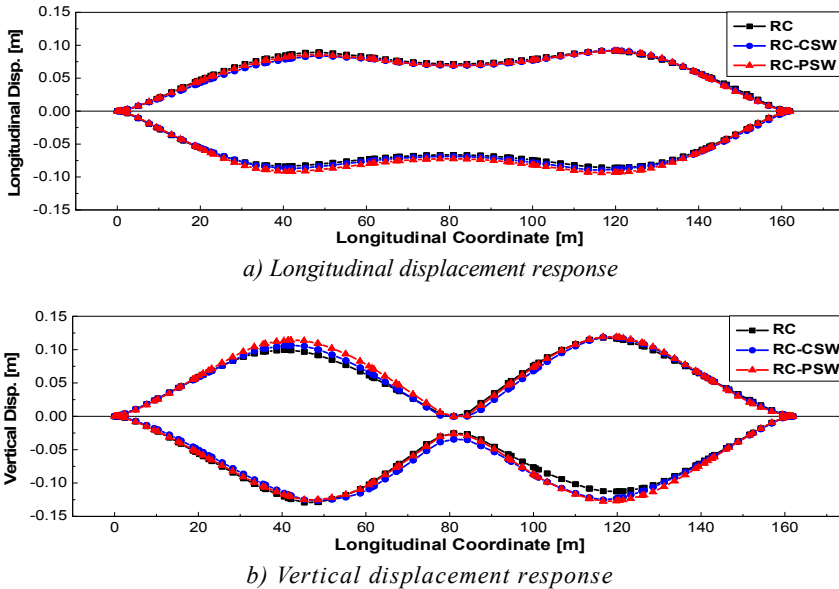


Fig. 12. Extremum of in-plane displacement response of arch ring under longitudinal earthquake.

3.2.3. Structural response under bi-directional seismic excitation

In this section, the same ground motions are applied simultaneously to the three arch bridges in transverse and longitudinal directions to investigate the structural responses against multi-dimensional earthquake excitations, and the resulting internal forces at the arch springing section are shown in Tab. 2. It is found that the combined excitations lead to a considerably greater axial force than those cases under individual excitation, either in transverse or longitudinal direction. However, for all the three arch bridges, there are no substantial differences in terms of out-of-plane bending moments between bi-directional and transverse excitations; however, the in-plane bending moments under longitudinal seismic excitations are greater than those under bi-directional seismic excitations.

As stated previously, the seismic responses of the arch bridges under transverse seismic excitations are greater than those under longitudinal seismic excitations, thus Tab. 3 only presents the ratio of the maximum strain at the outermost edge of the arch springing section under bi-directional and longitudinal seismic excitations, which is 1.17, 0.99, and 1.02 for RC, RC-CSW, and RC-PSW arch bridges, respectively. Therefore, the bi-directional loading effect on the nonlinear seismic responses of RC arch bridge shall be taken into account, while for RC-CSW and RC-PSW arch bridges it needs further study.

Table 2. Maximum of internal forces at the arch springing section.

Bridge types	Internal forces	Bi-directional f_1	Transverse f_2	Longitudinal f_3	f_1/f_2	f_1/f_3
RC	N [kN]	-66938	-55408	-58639	1.21	1.14
	Mz [kN*m]	196972	186466	2992	1.06	65.83
	My [kN*m]	53799	6608	62657	8.14	0.86
RC-CSW	N [kN]	-58501	-44825	-50220	1.31	1.16
	Mz [kN*m]	184301	181300	2934	1.02	62.82
	My [kN*m]	56034	13201	59838	4.24	0.94
RC-PSW	N [kN]	-59458	-45182	-53635	1.32	1.11
	Mz [kN*m]	229512	229677	1840	1.00	124.73
	My [kN*m]	44394	10460	58085	4.24	0.76

Table 3. Maximum strain at the outermost edge of the arch springing position.

Bridge types	Bi-directional ϵ_{xz}	Longitudinal ϵ_z	ϵ_{xz}/ϵ_z
RC	0.0188	0.0161	1.17
RC-CSW	0.0108	0.0109	0.99
RC-PSW	0.0080	0.0078	1.02

4. CONCLUSIONS

The main conclusions of this paper can be summarized as follow:

The axial force and out-of-plane bending moment are the predominant internal forces of arch bridges under transverse seismic excitations, and the arch springing sections of the three bridges have all reached the elastoplastic state; on the other hand, the axial force and in-plane bending moment are the predominant internal forces under longitudinal seismic excitations, and all the three arch bridges still remain in the elastic state. The seismic responses under transverse seismic excitations are greater than those under longitudinal seismic excitations.

The bi-directional loading effect, i.e. in both transverse and longitudinal directions, on the seismic responses of RC arch bridge shall be taken into account in the nonlinear analysis, while for RC-CSW and RC-PSW arch bridges it needs further study.

By comparing the maximum of internal forces and strains at the arch springing section and the displacement responses of the arch ring under different seismic excitations, RC-PSW arch bridges have better seismic performances than conventional RC arch bridge.

REFERENCES

- [1] CHEN B.C., WU Q.X., Wang Y.Y., Seismic response analysis of concrete arch bridge with corrugated steel webs, *Journal of Earthquake Engineering and Engineering Vibration*, Vol. 27, No. 3, 2007, pp. 47-53.
- [2] HUANG Q.W., CHEN B.C., Trial design for concrete arch bridge with corrugated steel webs, *Journal of Harbin Institute of Technology*, Vol. 39, No. Suppl. 2, 2007, pp. 686-689.

- [3] HUANG Q.W., CHEN B.C., Trial-design on a 160m-span concrete arch bridge with corrugated steel webs, *Journal of China & Foreign Highway*, No.2, 2007, pp. 78-83.
- [4] WU Q.X., CHEN B.C., WEI J.G., A geometric nonlinear finite element analysis for 3D framed structures, *Engineering Mechanics*, Vol. 24, No. 12, 2007, pp. 19-24.
- [5] WU Q.X., YOSHIMURA M., TAKAHASHI K., et al., nonlinear seismic analysis of the Second Saikai Bridge - concrete filled tubular (CFT) arch bridge, *Engineering Structures*, 28(2), 2006, pp. 163-182.
- [6] WU Q.X., CHEN B.C., TAKAHASHI K., Nonlinear seismic analysis of New Saikai Bridge, *Journal of Earthquake Engineering and Engineering Vibration*, Vol. 28, No. 5, 2008, pp. 55-64.
- [7] JAPAN ROAD ASSOCIATION, *Design Specifications for Highway Bridges - Part V: Seismic Design*, Maruzen Press, Tokyo, 2012.
- [8] REN W.X., OBATA M. Elastic-plastic seismic behaviour of long span cable-stayed bridges, *ASCE Journal of Bridge Engineering*, Vol. 4, No. 3, 1999, pp. 194-203.